Raman Microscopic Characterization of Proton-Irradiated Polycrystalline Diamond Films

R.L. Newton[a*], J.L. Davidson[b], M. J. Lance[c]

[a] Marshall Space Flight Center, Huntsville, AL
[b] Vanderbilt University, Nashville, TN
[c] Oak Ridge National Laboratory, Oak Ridge, TN
* Corresponding author email: *robby.newton@nasa.gov*

Abstract

The microstructural effects of irradiating polycrystalline diamond films with proton dosages ranging from 10^{15} to 10^{17} H^+/cm^2 was examined. Scanning Electron Microscopy and Raman microscopy were used to examine the changes in the diamond crystalline lattice as a function of depth. Results indicate that the diamond lattice is retained, even at maximum irradiation levels.

Introduction

Diamond possesses many of the most sought after material properties desired in present day applications; extreme hardness, high wear resistance, chemical inertness, optical transparency, and a wide band-gap. Crystalline diamond has the highest elastic modulus and hardness values known [1]. Polycrystalline diamond produced by techniques such as chemical vapor deposition (CVD) continue to show great promise for insertion into advanced technologies such as electronics, Microsystems (MST) and Microelectromechanical Systems (MEMS).

The fact that diamond is extremely resistant to radiation damage is an additional and potentially very important attribute of this material, especially for space-related applications where high radiation levels may be the norm. The effects of radiation on the properties of diamond have been studied for decades. However, the majority of these investigations have examined single crystal diamond, usually using heavy ions[2],[3]. Fewer studies have examined the effects of light ions, such as protons, on the microstructural changes of irradiated CVD diamond, particularly the microstructural changes as a function of ion implantation depth[4]. Also, polycrystalline diamond has not received as much attention as single crystal diamond despite its greater practical use. In this paper, we present the results of studies on the microstructural changes in proton-irradiated polycrystalline CVD diamond films.

Experimental

Polycrystalline diamond of approximately 20 microns in thickness was prepared on a 2" single crystal silicon substrate using microwave plasma assisted chemical vapor deposition (MPACVD) at a temperature of 800°C and a pressure of 110 Torr. The samples were implanted with protons using a NEC Model 5SDH-2 Pelletron accelerator at ambient temperature. Peltier cooling units were used to prevent overheating of the samples during the irradiation cycle. 600 keV protons were implanted at dosages that ranged from $2x10^{15}$ - $2x10^{17}$ H^+/cm^2 at 1.2-6.0$x10^{-7}$ Torr. The samples were not annealed after the irradiation exposure. Scanning Electron Microscopy (SEM) micrographs of the specimens were taken using an Electroscan Environmental SEM (FEI Inc., Hillsboro, OR).

Raman Microscopy was used to determine the crystalline integrity of the diamond films. A Dilor XY800 Raman microprobe (JY, Inc., Edison, NJ) configured as a single stage spectrograph using a microscope with a ~1 micron spatial resolution was used in conjunction with an Innova 308C Ar+ ion laser (Coherent, Inc., Santa Clara, CA) at 514.5 nm and 100 mW output power to collect spectra. The

system was set up to automatically map changes in the diamond spectra moving away from the surface of the film collecting a spectrum every 1 micron. Samples were broken to provide pristine cross-sections for analysis of ion penetration depth. The penetration depth was approximately 2 μm. A combination Gaussian-Lorentzian function was used for curve fitting.

Results

While there were no apparent visible changes in the $2x10^{15}$ H^+/cm^2 implant, the surfaces of the remaining diamond films were darkened with increasing proton dosage. The most heavily irradiated film displayed areas of a dark brown discoloration. For brevity, detailed experimental results will only be presented for the as-deposited and most heavily irradiated specimens.

Top Surface Analysis

SEM analysis of the top surface of the as-deposited specimen indicated a <111> crystal growth with large facets. The grains are on the order of several microns in diameter with sharp, well defined edges, as shown in Fig. 1(a) In contrast to the as-deposited specimens, the SEM micrograph of the top surface of most heavily irradiated specimen ($2x10^{17}$ H^+/cm^2) showed significant damage (Fig. 1(b)). The surface was severely discolored, with noticeable disruption of the crystallite edges.

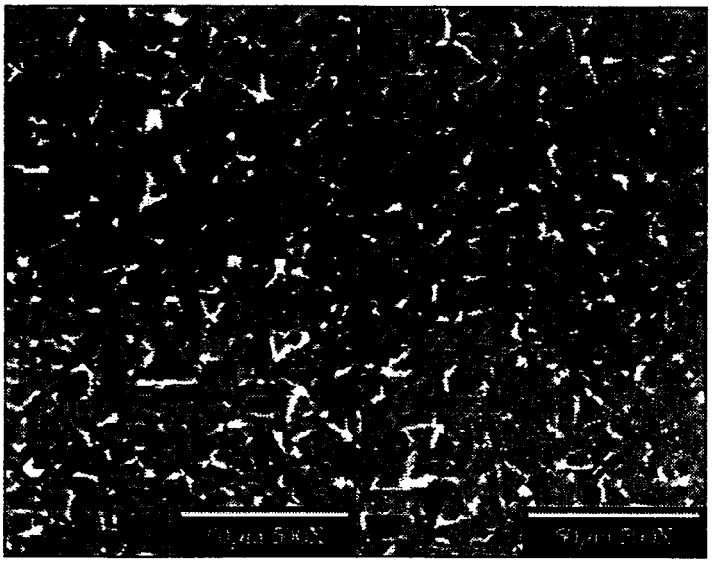

Figure 1. SEM micrograph of the top surface of as-deposited (a) and the heavily irradiated (b) polycrystalline diamond films.

Three Raman spectra from the top surface of each specimen were collected, normalized and averaged. Figure 2 shows a typical spectrum from the as-deposited specimen with the inset showing the curvefit. Single crystal diamond exhibits a sharp Raman peak at 1333 cm^{-1} with a full width at half maximum (FWHM) of less than 3.0 with no other spectral signatures present. As Fig. 2 indicates, the as-deposited material compared extremely well with high purity single crystal material, although the diamond used in this study was polycrystalline. The diamond peak is sharp, well defined, and symmetrical. The FWHM is close to that reported for high-purity single crystal diamond. No graphitic or amorphous bands are observed.

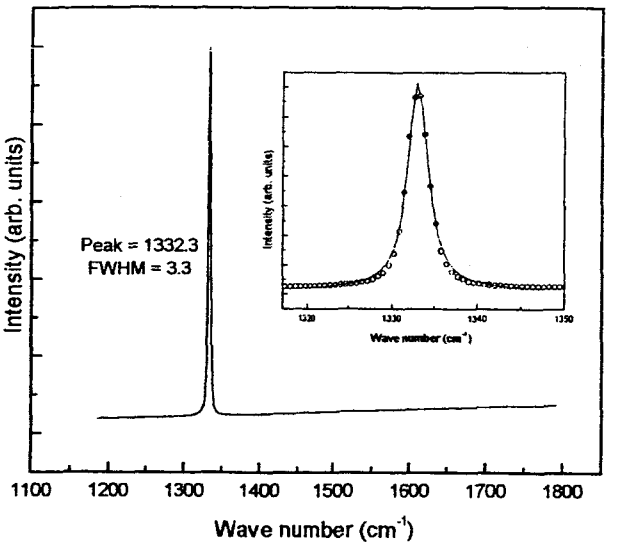

Figure 2. Raman spectrum of the top surface of as-deposited polycrystalline diamond wafer. Inset shows a Lorentizian curvefit of the peak.

The Raman spectra taken from the top surface of the most heavily irradiated specimen indicates extensive ion-induced damage to the microstructure as shown in Figure 3. Due to darkening of the surface of the specimen, the probe depth of the Raman signal was attenuated in comparison to the as-deposited samples. The first-order diamond peak is shifted downward by almost two wave numbers and the intensity of the peak is greatly diminished. Peaks attributed to ion implantation damage – i.e. the monovacancy (1490 cm^{-1}), the split interstitial (1630 cm^{-1}), and the broad graphitic band at ~1550 cm^{-1}, are observed and coincided with the broadening of the first-order diamond peak. Other broad damage peaks are also observed.

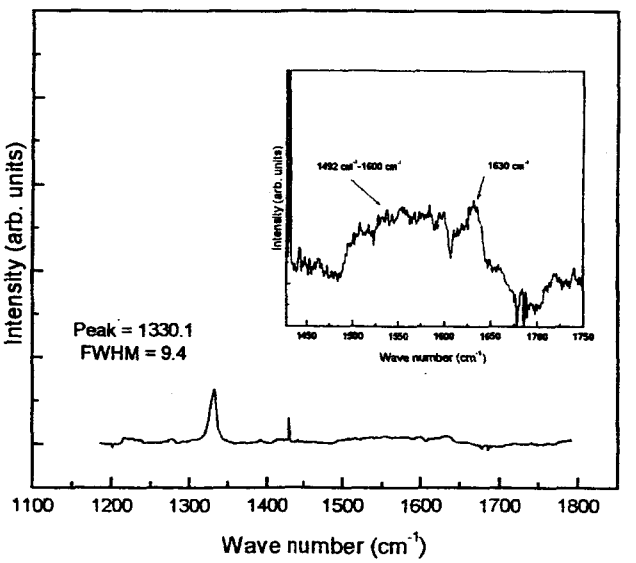

Figure 3. Raman spectra from top surface of $2x10^{17}$ H^+/cm^2 implanted polycrystalline diamond wafer. Implantation induced damage is shown in the inset.

Cross Section Analysis

SEM edge analysis of the cleaved edge of the as-deposited material revealed an extremely rough edge surface as shown in Fig. 4(a). The interface of the diamond film/silicon substrate is clearly evident. Columnar growth, typically seen in <111> diamond films, is difficult to detect in this specimen. The SEM edge view of the $2x10^{17}$ H^+/cm^2 implant is shown on the right side of Fig. 4. No effect of the proton implant is observed.

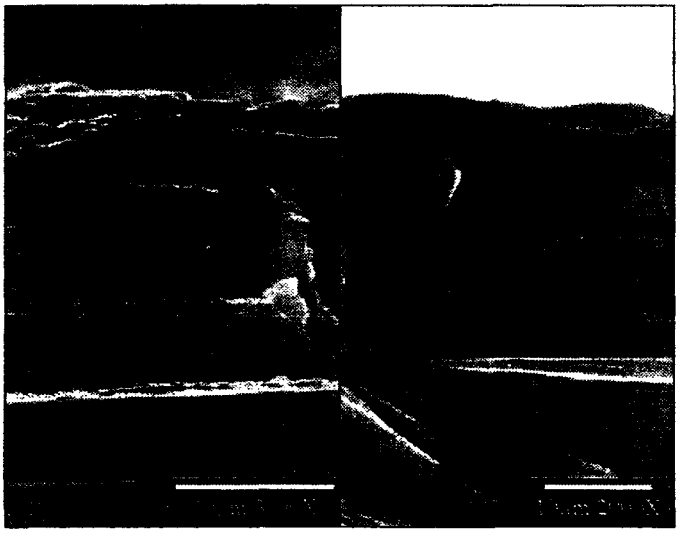

Figure 4. SEM micrograph showing the edge surface of the as-deposited film (a) and the heavily irradiated (b) polycrystalline diamond wafer films.

The cross-sectional Raman spectra for the as-deposited material is shown in Figure 5. The spectrum from the first micron contains a sharp first-order diamond peak at ~1332 cm^{-1}, and a broad band from ~1450 cm^{-1} to 1700 cm^{-1}, which is indicative of graphitic-like carbon. This is attributed to surface effects where carbon exists in a variety of bonding configurations. The spectra 2-6 microns away from the surface are devoid of this broad peak signifying the high fidelity of the carbon film throughout the entire layer. This material is essentially free of depth-dependent stress and microstructural damage due to the fact that the first-order diamond peak shifted little and there was no increase in the FWHM.

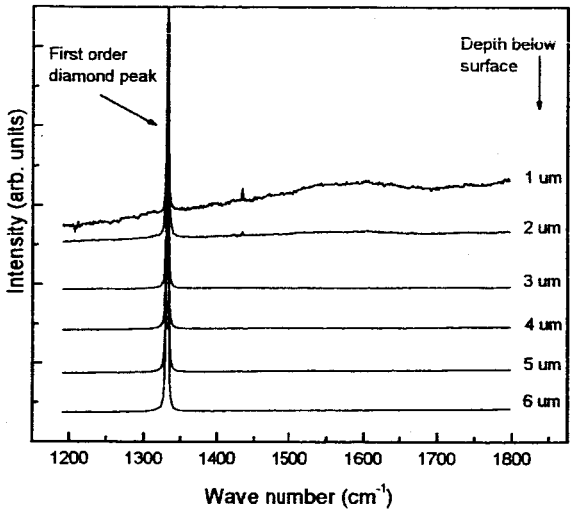

Figure 5. Raman spectra as a function of depth of the as-deposited polycrystalline diamond film.

The cross-sectional Raman analysis of the proton implantation as a function of depth for the $2x10^{17}$ H^+/cm^2 implanted sample is presented in Fig. 6. In this representative line scan, extensive defect-related spectral signatures are evident. The vacancy (1495 cm^{-1}), the broad amorphous region at ~1550 cm^{-1}, and the <100> split interstitial (1630 cm^{-1}) are all present at 1 μm. The first-order Raman line is greatly diminished in intensity as compared to the as-deposited sample. The damage increases until reaching a maximum at 4 microns. At this depth, the 1333 cm^{-1} diamond peak is diminished in intensity but still present. The 1495 cm^{-1} peak may be present but resolution is difficult due to the increase in baseline present throughout the entire region. The 1630 cm^{-1} peak grows in intensity as a function of depth until reaching a maximum at 4 microns. By 6 microns, the spectra returned in appearance to the as-deposited specimen, although the baseline is still slightly elevated across the entire 1400 cm^{-1} to 1650 cm^{-1} region.

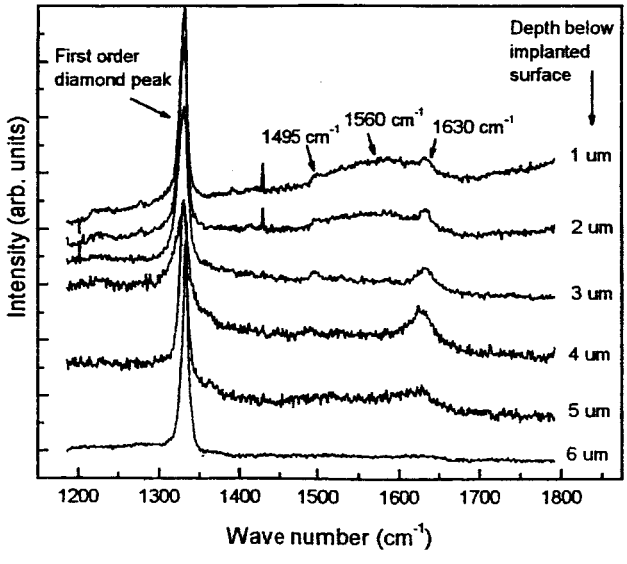

Figure 6. Raman spectra as a function of depth for the $2x10^{17}$ H^+/cm^2 proton implanted polycrystalline diamond film.

Discussion

The spatial distribution of defects caused by proton implantation was modeled using The Stopping and Range of Ions in Matter (SRIM), which calculates damage (i.e. vacancies, interstitials, and knock-on atoms) as a function of implantation depth in the material [5]. As can be seen in Fig. 7, the calculated concentration of vacancies reaches a maximum at ~3.6 microns in depth. As Fig. 6 indicates, based on the observed changes in microstructure as a function of depth, SRIM accurately predicts the maximum depth (i.e. the End-of-Range or EOR) for the implanted protons into the diamond films within the experimental error (~1 micron).

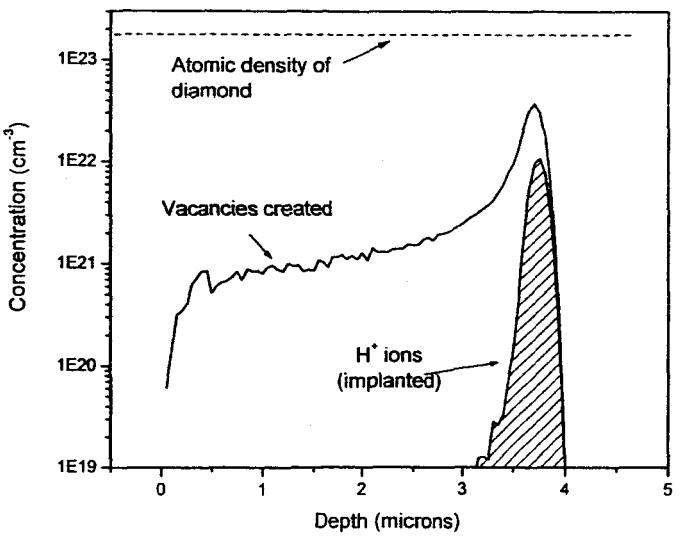

Figure 7. Spatial distribution of radiation damage in diamond implanted with 600keV protons using SRIM analysis.

The cross-sectional sample configuration used throughout these experiments provided optimum conditions for theoretical and experimental comparisons. The top surface of the most heavily irradiated specimen showed a significant shift in both first order diamond peak position and FWHM. Due to the fact that that the diamond line shape was symmetric rather than skewed, the defects were considered to be localized in the form of point defects. The downshift in peak position is indicative of tensile stress in the material.

In the two more heavily irradiated specimens, the near surface damage was greater than that predicted using TRIM. This is consistent with other ion implantation studies with diamond material (mainly single crystal) in which more surface damage was observed than was predicted using TRIM software[6]. This study indicates this to be the case in polycrystalline diamond as well. Examination of Fig. 6 provides evidence of defect-related near surface damage. In addition to the spectra containing graphitic-like components at ~1580 cm^{-1}, defect-related damage was also indicated at 1495 cm^{-1} and 1630 cm^{-1}.

The first order diamond peak position as a function of depth is presented in Fig. 8 for the entire experimental series. No implantation induced effects, within experimental error, were observed in the 2 x10^{15} H^+/cm^2 implant at any depth. However, both the 2x10^{16} and 2x10^{17} H^+/cm^2 dosages caused measurable shifts in the first order diamond peak position, although at 10 microns both specimens had returned to as-deposited peak position values.

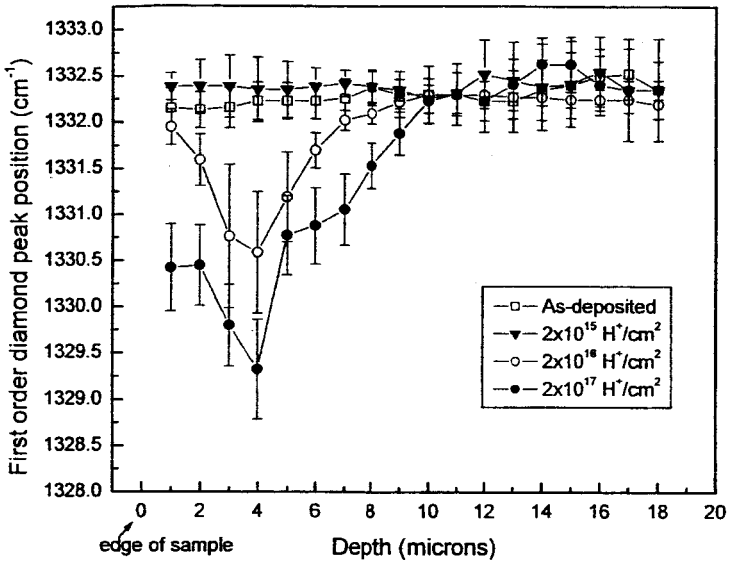

Figure 8. The variation in first order peak position as a function of depth for the entire implantation series.

In a similar fashion, the first order diamond peak FWHM for all samples are presented in Fig. 9. Again, no apparent effects from the implantation are observed for the 2x10^{15} H^+/cm^2 implant. The 2x10^{16} and 2x10^{17} H^+/cm^2 specimens behaved in similar fashion. Both increased rapidly until reaching the End-of-Range (EOR) and then decreased slowly until approximately 10 microns, where the values returned to baseline behavior as in the control specimen.

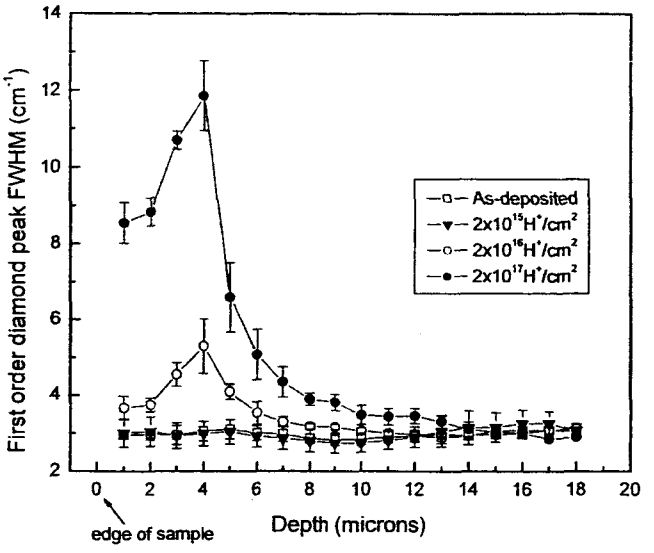

Figure 9. Variation in first order FWHM as a function of depth for the entire implantation series.

According to the Raman spectra, the main defect structure at the EOR for the protons is the 1630 cm^{-1} split interstitial. The behavior of this defect is in agreement with present theory in that the peak is expected to increase with increasing dosage[7]. The other main defect observed, the 1490 cm^{-1} vacancy, showed a decrease with increasing dosage.

While the EOR is very narrow (~0.5 microns) the first order diamond peak position in both the $2x10^{16}$ H^+/cm^2 and the $2x10^{17}$ H^+/cm^2 dosed specimens does not return to as-deposited values (i.e. baseline) for some 6 additional microns beyond the implant region. This slow return to baseline has been observed in prior study of ^{13}C implanted natural diamond. Spits, et al. observed a similar "tailing" behavior by using the resonant nuclear reaction ^{13}C 9p, (gamma) ^{14}N at 550 keV [8]. They discovered that the depth to which the tail penetrates appears to increase with decreasing temperature. They concluded that interstitials are forced out of the implanted area (under high strain) into the bulk. In the present study, the presence of grain boundaries in the material apparently did not serve as a barrier of sink to this carbon atom interstitial migration.

Conclusion

The depth-dependent Raman spectra for the as-deposited diamond film demonstrates the efficacy of film fabrication using the microwave plasma assisted chemical vapor deposition method (MPACVD). Near the surface, small amounts of graphitic carbon were detected. This is to be expected, however, as a result of film growth termination. At all remaining depths, the diamond was devoid of graphitic carbon. The first order diamond peak was intense and stress free.

Three different diamond films were implanted with varying doses of protons. A visual inspection of the films after implantation revealed a noticeable darkening of the two more highly implanted specimens, that being the $2x10^{16}$ H^+/cm^2 and $2x10^{17}$ H^+/cm^2 implants. SEM analysis of the top surface showed a small amount of darkening in some locations in the $2x10^{16}$ H^+/cm^2 implanted films with extensive surface damage and heavy discoloration in the $2x10^{17}$ H^+/cm^2 films. Cross-sectional SEM analysis of the specimens failed to reveal any obvious effects of the implantation at any depth.

Much information was collected from the Raman data. Due to the downward shift in the first-order diamond peak, the $2x10^{16}$ H^+/cm^2 and $2x10^{17}$ H^+/cm^2 implanted films were shown to be under tensile stress. This stress reached a maximum near the EOR for the protons, that being approximately 4 microns from the surface. The broadening of the peak correlated with the implant dosages. This indicated a high degree of damage. This damage was confirmed by the presence of the vacancy and the <100> split interstitial being detected in the Raman spectra.

An interesting observation was noted in the Raman data. The stress created by the implantation process extended well into un-irradiated material and did not return to a baseline until reaching a depth of approximately 2x(EOR). This observation has been noted before in single crystal diamond. This is attributed to interstitials being forced into the bulk due to stress. Based on the results on the present investigation, polycrystalline diamond films may be suitable for applications where microstructural resistance to radiation effects are of utmost importance.

Acknowledgments

This work was supported by NASA's Marshall Space Flight Center. MJL sponsored by the Division of Materials Sciences and Engineering, U. S. Department of Energy, under Contract DE-AC05-00OR22725 with UT-Battelle, LLC. Special thanks to Mr. Charles Griffith of MSFC for sample preparation and Mr. Jimmy Coston of MSFC for the SEM analysis.

References

[1] J.P. Sullivan, T.A. Friedmann, and K. Hjoit, MRS Bulletin, April, (2001) 309.
[2] D.N. Jamieson, S. Prawer, K.W. Nugent, and S.P. Dooley, Nucl. Instr. Meth. B106, (1995) 641.
[3] J.O. Orwa, K.W. Nugent, , D.N. Jamieson, and S. Prawer, Phys. Rev. B62, (2000) 5461.
[4] A.A. Gippius, R.A. Khmelnitsky, V.A. Dravin, and A.V. Khomich, Physica B 308-310, (2001) 573.
[5] J.F. Ziegler, J.P. Biersack and U. Littmark, The Stopping and Range of Ions in Solids (Pergamon, New York, 1985).
[6] G. Ramos and B.M.U. Scherzer, Nucl. Instr. Meth. B174, (2001) 329.
[7] J.F. Prins, J. Phys. D: Appl. Phys. 34, (2001) 3003.
[8] R.A. Spits, T.E. Derry, J.F. Prins, , and J.P.F. Sellschop, Nucl. Instr. Meth. B51, (1990) 247.